PHYSICAL REVIEW C **75**, 032801(R) (2007)

Precise measurement of the ^{64}Ge mass and its effect on the *rp* process

J. A. Clark,[1,2,3] K. S. Sharma,[2] G. Savard,[3,4] A. F. Levand,[3] J. C. Wang,[2,3] Z. Zhou,[3] B. Blank,[3,5] F. Buchinger,[6] J. E. Crawford,[6] S. Gulick,[6] J. K. P. Lee,[6] D. Seweryniak,[3] and W. Trimble[3]

[1]*Wright Nuclear Structure Laboratory, Yale University, New Haven, Connecticut 06520, USA*

[2]*Department of Physics and Astronomy, University of Manitoba, Winnipeg, Manitoba R3T 2N2, Canada*

[3]*Physics Division, Argonne National Laboratory, Argonne, Illinois 60439, USA*

[4]*Department of Physics, University of Chicago, Chicago, Illinois 60637, USA*

[5]*Centre d'Etudes Nucléaires de Bordeaux-Gradignan, F-33175 Gradignan Cedex, France*

[6]*Department of Physics, McGill University, Montreal, Quebec H3A 2T8, Canada*

(Received 29 April 2006; published 21 March 2007)

The Canadian Penning Trap mass spectrometer has been used to determine the mass excesses of ^{64}Ge and ^{64}Ga as −54344(30) keV and −58832.5(39) keV, respectively. Under typical conditions used for modeling x-ray bursts, ^{64}Ge is confirmed as a waiting-point nuclide and can contribute up to 35.5 s to the timescale of the *rp* process at a peak x-ray burst temperature of 1.5 GK.

DOI: 10.1103/PhysRevC.75.032801 PACS number(s): 26.30.+k, 21.10.Dr, 27.50.+e, 98.80.Ft

Binary star systems each consisting of a gas giant and neutron star are possible sources for observed x-ray bursts. If hydrogen and helium from the gas giant can accrete onto the surface of the neutron star at a rate of $\sim 10^{-9} M_{\odot}\mathrm{yr}^{-1}$, where $M_{\odot} \equiv 1$ solar mass, the accreted material is subjected to an ever-increasing change in pressure and temperature until fusion of the material becomes possible [1]. At this point the accumulated material burns rapidly and results in a thermonuclear runaway [2] with temperatures reaching up to 3×10^9 K. At this time, the nuclear energy released during the rapid series of proton capture reactions, termed the *rp* process [3], is sufficient to be observed above the relatively constant accretion background. The resulting burst of energy is ultimately observed as an x-ray burst [4] with a typical duration of 10 to 100 s.

During thermonuclear runaway, the reaction path is dictated by thousands of reaction rates, including those of predominant proton capture, photodisintegration, and β decay. In the temperature regime during an x-ray burst, β decay often occurs less frequently than proton capture or photodisintegration. Therefore, the *rp* process proceeds by a series of rapid-proton capture reactions until reaching a "waiting-point" nuclide where the inverse photodisintegration reaction rate is comparable to the proton-capture rate. The *rp* process essentially stalls and cannot continue until the nucleus is destroyed, either through its β decay, or through the rapid capture of two protons to bypass the impeding nucleus. Another series of reactions then ensues until the next waiting-point nuclide is reached, and the process continues in this manner until it terminates in the Sn-Sb-Te region [5]. The timescale of the *rp* process, or equivalently the light-curve profile of x-ray bursts, depends largely upon the contribution of the individual delays at each waiting-point nuclide [6]. Since these delays are dependent upon the reaction rates of the nuclides involved, information about β-decay half-lives and energy levels which can be thermally populated are necessary to assess the delay at each waiting-point nuclide. Furthermore, since the photodisintegration rates are exponentially dependent upon differences in the masses of the nuclides involved [1], masses of potential waiting-point nuclides are critical.

Since the delay in the *rp* process from any waiting-point nuclide can be at most equal to its β-decay lifetime, the waiting-point nuclides which could have the biggest influence are those with the longest β-decay lifetimes, in particular ^{64}Ge and ^{68}Se, with β-decay half-lives of 63.7 s and 35.5 s, respectively [1,5,7–9]. The mass of ^{68}Se has been measured previously and found to contribute significantly to the total timescale of the *rp* process [10]. In this Rapid Communication we report a mass measurement of ^{64}Ge and its effect on the astrophysical *rp* process.

A brief description of the Canadian Penning Trap (CPT) mass spectrometer and details specific to this paper are presented here. Further information regarding the apparatus can be found elsewhere [11,12]. The isotopes ^{64}Ge, ^{64}Ga, and ^{64}Zn were produced in fusion-evaporation reactions between a 185 MeV ^{54}Fe beam and carbon targets of 1 mg cm^{-2} mounted on a rotating target wheel. The evaporation residues were focused and separated from the primary beam before entering a gas catcher [13] where the ions were thermalized in helium gas. These ions, together with molecular ions created along the ionization tracks of the evaporation residues, were subsequently extracted and subjected to a mass selective cooling process [14] within a gas-filled Penning trap. The selected ions were then transferred to a linear RF quadrupole ion trap (RFQ) which was used to accumulate and cool the ions prior to injection into the precision Penning trap for the mass measurement.

An ion of mass m and charge q is confined in a Penning trap by the superposition of magnetic and electric fields. The central, or ring, electrode of the Penning trap is divided into quadrants to enable the application of azimuthally oscillating quadrupole potentials superimposed on the static trapping potential. The influence of a quadrupole excitation results in a resonance at the cyclotron frequency, $\omega_c = qB/m$, [15,16] where B represents the strength of the homogeneous magnetic field.

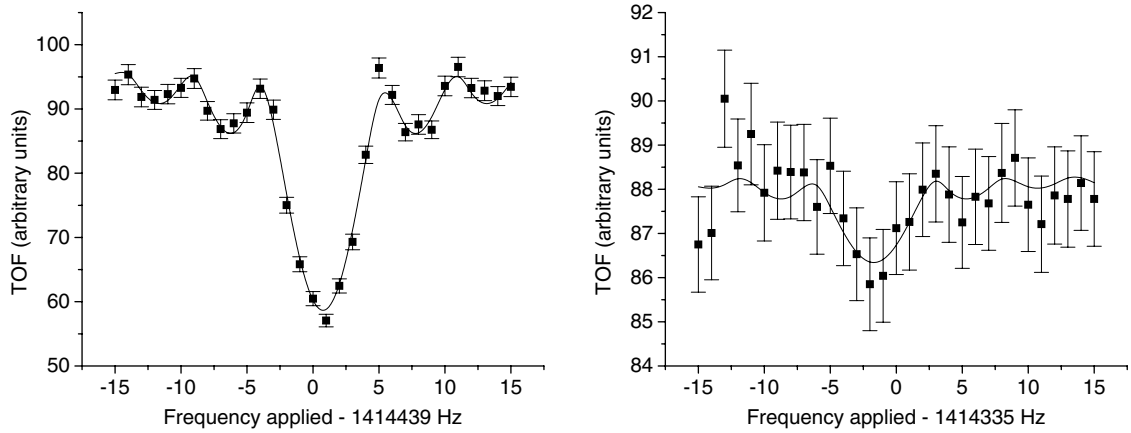

FIG. 1. A TOF spectrum obtained for $^{64}Ga^{+}$ (left) and $^{64}Ge^{+}$ (right). Quadrupole excitations of 200 ms in duration were applied after first removing contaminant ions and establishing an initial orbital radius. Both spectra have a FWHM of ∼4.5 Hz (190 keV) which is consistent with the Fourier limit. The reduction in the TOF depth for $^{64}Ge^{+}$ as compared to $^{64}Ga^{+}$ is due to the presence of contaminant ions remaining after the purification process.

The cyclotron frequency of these ions is determined using the time-of-flight (TOF) technique [17]. After the excitation frequency has been applied for a prescribed exposure, the ions are ejected from the trap. The radial energy gained from the excitation is then converted into axial energy by their passage through the magnetic field gradient outside the Penning trap. The TOF corresponding to the ions' arrival at a microchannel plate detector is recorded with a multichannel scaler. A TOF spectrum is then generated by plotting the mean TOF of the ions as a function of the driving frequency. The resonant frequency, ω_c, is obtained by determining the position of the minimum of the TOF spectrum.

The masses of ^{64}Ge and ^{64}Ga reported here were determined from two experiments. During the first experiment, the cyclotron frequency ratio between $^{64}Ga^{+}$ and $^{64}Zn^{+}$ was obtained. On average, three ions of $^{64}Ga^{+}$ and 0.5 ions of $^{64}Zn^{+}$ were detected at the microchannel plate TOF detector after each respective measurement cycle. The duration of each cycle, which includes the time needed to remove most contaminant ions, establish an initial orbital radius, and the subsequent quadrupole field excitation, was typically 0.75 s. The second run provided cyclotron frequency ratios of $^{64}Ge^{+}$ and $^{64}Ga^{+}$ relative to $^{64}Zn^{+}$. In this second experiment, TOF spectra of $^{64}Ga^{+}$ and $^{64}Zn^{+}$ were generated with on average two ions detected per cycle, and $^{64}Ge^{+}$ spectra consisted of 0.7 ions detected on average per cycle, with approximately 95% of the 0.7 ions being due to contaminant ions remaining from the purification process. Although this cleaning process is approximately 95% efficient, some $A = 64$ ions remain due to the overwhelming production of molecular ions in the gas catcher. The dominant effect resulting from the presence of contaminant ions is a reduction in the TOF amplitude. As discussed later, a shift in the cyclotron frequency due to interactions with contaminant ions is also possible but we find this effect to be essentially negligible when so few ions are stored at a time in the trap. Sample TOF spectra for $^{64}Ga^{+}$ and $^{64}Ge^{+}$ are shown in Fig. 1. In addition to the 200 ms quadrupole field excitations for all mass $A = 64$ ions studied, one TOF spectrum each of $^{64}Zn^{+}$ and $^{64}Ga^{+}$ was obtained with quadrupole field excitations of 400 ms in duration during the second experiment.

The final cyclotron frequency ratio, R, between singly-charged ^{64}Ga and ^{64}Zn ions was determined to be 1.000120423(50) while that between singly-charged ^{64}Ge and ^{64}Zn ions was 1.00019580(51), where the uncertainties are of statistical nature only. A discussion of the effects of known sources of systematic errors [15] which were examined during the course of each measurement follows. Any potential systematic bias proportional to the difference in mass between the reference and measured species is negligible, as the mass difference between ^{64}Zn and ^{64}Ge is only 0.012 u. Previous measurements [18] indicate that any such effect is typically less than $10^{-9}u^{-1}$. Effects due to ion-ion interactions were minimized by keeping a small number of ions in the trap during the quadrupole excitation. The largest difference in the number of ions detected per measurement cycle between ion species was ∼4 which results in a systematic uncertainty of 8 ppb [19–21]. A systematic effect which is comparable in magnitude is due to the presence of contaminant ions. An estimate of the magnitude of this effect is derived in Ref. [20]. In that paper, after corrections were made for all other systematic effects, the remaining differences in the mass determinations between the CPT and the 2003 atomic mass evaluation ('03 AME) [22] for precisely known nuclides was $\Delta m \sim 1 \times 10^{-8} \cdot m$. This remaining systematic uncertainty could possibly be due to the presence of contaminant ions, and since the conditions for that experiment and the ^{64}Ge experiment are similar in terms of the number of simultaneously trapped ions, the uncertainty $\Delta m/m \sim 1 \times 10^{-8}$ is used as an estimate for the effect from contaminant ions. Possible variations in the magnetic field strength with time were monitored by watching for fluctuations in ω_c for $^{64}Zn^{+}$ and $^{64}Ga^{+}$. Although no shifts in the measured frequencies (within the precision of our measurements) was observed, we expect a slow decay of the magnetic field of magnitude $(\Delta B/B)$ no greater than 8×10^{-10} hr^{-1} [20,21]. We therefore include a systematic uncertainty of 38 ppb due

TABLE I. Atomic masses with combined statistical and systematic uncertainty, the resulting mass excesses, and comparisons with the '95 AME [24] and FRDM [25].

Nuclide	Mass (μu) This paper	Mass excess (keV)		
		This paper	'95 AME	FRDM
^{64}Ga	63936840.7(42)	−58832.5(39)	−58835(4)	−57650
^{64}Ge	63941660(32)	−54344(30)	−54420(250)	−53040

to magnetic field decay over the typical two-day period of each experiment. Finally, the total systematic uncertainty for the ^{64}Ge experiments is obtained by summing the individual contributions of systematic uncertainty in quadrature and the final uncertainty is a combination of the statistical uncertainty and this systematic error ($\Delta m/m = 4 \times 10^{-8}$) added in quadrature.

For each cyclotron frequency ratio R, the mass of the neutral isotope, m, is determined using the relationship $m = R(m_c - m_e) + m_e$ where m_e is the mass of the electron and m_c is the mass of the neutral reference mass, ^{64}Zn. The values for m_e and m_c, along with other auxiliary data, were extracted from Refs. [22,23] and combined with our cyclotron frequency ratios to arrive at the results shown in Table I. The '03 AME already incorporates preliminary results from this work, so we compare in Table I our values to the 1995 atomic mass evaluation ('95 AME) [24] instead and the finite-range droplet model (FRDM) [25] predictions. Good agreement exists with the '95 AME, but the experimental results show that ^{64}Ga and ^{64}Ge are more bound by 1243 keV on average than predicted by the FRDM.

Although the ^{64}Ge mass excess reported here disagrees with the recent measurement from the SPEG facility [$\Delta(^{64}\text{Ge}) = -53180(640)$ keV] [26], our derived Q_{EC} value for ^{64}Ge [$Q_{EC} = \Delta(^{64}\text{Ge}) - \Delta(^{64}\text{Ga}) = 4489(30)$ keV] is in excellent agreement with the much older result of 4410(250) keV reported by Ref. [27]. The determination of the ^{64}Ga mass reported here is also in good agreement with the '03 AME which takes as inputs to the evaluation two experimental results. Furthermore, since the publication of the '03 AME, the mass of ^{64}Ga was measured by the CSS2 cyclotron at GANIL and the outcome of their experiment [$\Delta(^{64}\text{Ga}) = -58716(120)$ keV] [28] also agrees with our result.

The effect of our mass determination of ^{64}Ge on the effective stellar half-life of ^{64}Ge, $t_{1/2,\text{eff}}(^{64}\text{Ge})$, or equivalently the delay in the rp process at ^{64}Ge, is shown in Fig. 2. The plotted curve, which is generated with parameters approximating x-ray burst environments (temperature = 1.3 GK, density = 10^6 g cm^{-3}, and solar hydrogen abundance), shows the exponential dependence of the effective half-life of ^{64}Ge on the proton-capture Q value of ^{64}Ge, $Q_p(^{64}\text{Ge})$, as discussed in Ref. [1]. At temperatures at and below 1.3 GK, the photodisintegration of ^{66}Se can be neglected and an exit from the ^{64}Ge-^{65}As equilibrium can be accomplished via two-proton capture to ^{66}Se or β decay of ^{64}Ge. For small (even negative) Q_p values, the proton-capture rate on ^{64}Ge is small in comparison with the inverse photodisintegration rate. Therefore, bypassing ^{65}As by capturing two protons in

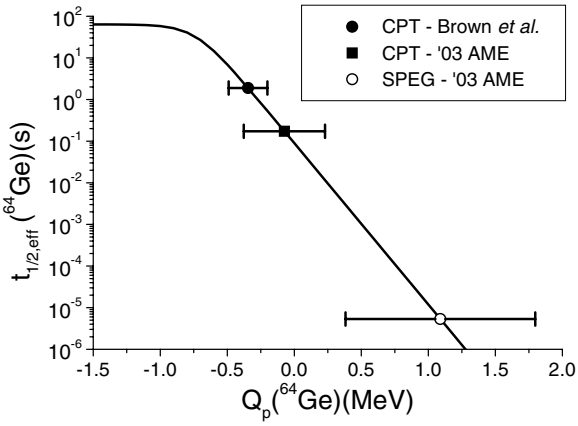

FIG. 2. The effective stellar half-life of ^{64}Ge as a function of $Q_p(^{64}\text{Ge})$. Each legend entry has two parts: the first part represents the values used for the mass of ^{64}Ge, and the second part indicates the value used for the mass of ^{65}As. The curve was generated using parameters approximating x-ray burst environments (see text).

rapid succession at these temperatures is highly improbable, and the rp process is delayed until the β decay of ^{64}Ge occurs. For larger Q_p values, the increased likelihood of destruction of ^{64}Ge via proton-capture decreases the effective half-life of ^{64}Ge since the rp process can bridge the intermediate nucleus, ^{65}As, and continue before the β decay of ^{64}Ge takes place.

Along the curve plotted in Fig. 2 are three $Q_p(^{64}\text{Ge})$ values determined with various inputs for the masses of ^{64}Ge and ^{65}As. If the value for $Q_p(^{64}\text{Ge})$ is determined using the mass of ^{64}Ge from SPEG and the ^{65}As mass from the '03 AME, the effective stellar half-life of ^{64}Ge is less than 1 ms. However, when our reported ^{64}Ge mass is combined with the calculations of Coulomb displacement energies from Brown *et al.* [8] and the mass of ^{65}Ge from Ref. [22] to yield $Q_p(^{64}\text{Ge}) = -345(140)$ keV, the effective stellar half-life of ^{64}Ge is between 0.5 and 7 s. Therefore, the rp process would seem to encounter a small delay at ^{64}Ge.

With temperatures exceeding 1.3 GK, the photodisintegration of ^{66}Se is not negligible and the waiting-point nuclide ^{64}Ge establishes an equilibrium with both ^{65}As and ^{66}Se. To examine more fully the temperature dependence of the effective delay the rp process path encounters at ^{64}Ge, a simple network code was generated which considers proton capture on ^{64}Ge and ^{65}As, photodisintegration of ^{65}As and ^{66}Se, and β decay of ^{64}Ge, ^{65}As, and ^{66}Se. For each temperature under consideration, the system of differential equations describing the abundances of ^{64}Ge, ^{65}As, and ^{66}Se were solved assuming constant density and temperature with time. Proton capture rates, photodisintegration rates, and partition functions were extracted from Ref. [29]. The new masses reported here were used to reevaluate the photodisintegration rates from Ref. [29]; however, no new proton capture rates were generated as the influence of the new masses on the proton capture rates in comparison is negligible. Beta-decay half-lives of 63.7 s, 170 ms, and 33 ms [30] were assumed for ^{64}Ge, ^{65}As, and ^{66}Se, respectively. The results from the code are shown in Fig. 3. As our measurements have already influenced the '03 AME, we prefer to delineate the range of lifetimes allowed

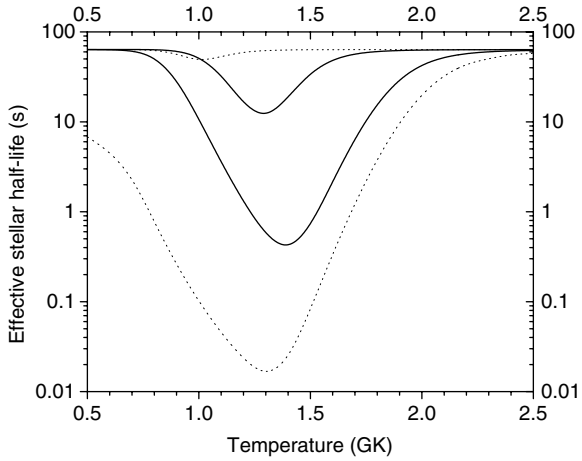

FIG. 3. The effective stellar half-life of ^{64}Ge as a function of temperature in the stellar environment. The dotted lines delineate the range of the effective stellar half-life allowed within the uncertainty of the '95 AME and the solid lines outline the possible range within the uncertainty of our measurements.

within the uncertainty of the '95 AME and compare this range to that resulting from our measurements. For each set of masses considered, the temperature dependence of the effective half-life of ^{64}Ge is clear. At low temperatures, the proton-capture rate is insufficient for ^{64}Ge to emerge from a ^{64}Ge-^{65}As equilibrium via two-proton capture to ^{66}Se, and ^{64}Ge must β decay before further proton captures are possible. At high temperatures, the photodisintegration rate of ^{66}Se overwhelms any proton-capture process forming ^{66}Se, and once again the rp-process can continue only through the β decay of ^{64}Ge. At intermediate temperatures, however, the creation of ^{66}Se by proton capture is more likely than the photodisintegration of ^{66}Se, and therefore the effective half-life of ^{64}Ge is decreased. The temperature window for which the effective half-life of ^{64}Ge is less than its β-decay half-life depends upon the proton-capture Q values. Notice from Fig. 3 the diminished uncertainty in the effective half-life solely due to our mass measurement of ^{64}Ge. In some temperature regimes, the uncertainty has been reduced by two or more orders of magnitude. At the very least, we find the effective half-life of ^{64}Ge to be no less than 0.4 s, confirming ^{64}Ge as a waiting-point nuclide. With an x-ray burst peak temperature of 1.5 GK, we estimate the effective half-life to be between 0.7 and 35.5 s.

The masses of the waiting-point nuclides with the longest β-decay lifetimes have now all been measured precisely. We improved the precision of the ^{64}Ge mass by an order of magnitude, and our result, when combined with the masses of ^{65}As and ^{66}Se determined from Coulomb displacement energies, confirms ^{64}Ge as a waiting-point nuclide under assumptions typically used in modeling x-ray bursts. A further reduction in the uncertainty of the effective half-life of ^{64}Ge would be achieved with a more precise mass determination of ^{65}As.

This work was supported by the U.S. Department of Energy, Nuclear Physics Division, under Contract No. W-31-109-ENG-38, and by the Natural Sciences and Engineering Research Council of Canada.

[1] H. Schatz, A. Aprahamian, J. Görres, M. Wiescher, T. Rauscher, J. F. Rembges, F.-K. Thielemann, B. Pfeiffer, P. Möller, K.-L. Kratz, H. Herndl, B. A. Brown, and H. Rebel, Phys. Rep. **294**, 167 (1998).

[2] M. Wiescher, J. Görres, and H. Schatz, J. Phys. G **25**, R133 (1999).

[3] R. K. Wallace and S. E. Woosley, Astrophys. J. Suppl. Ser. **45**, 389 (1981).

[4] T. Strohmayer and L. Bildsten, in *Compact Stellar X-Ray Sources*, edited by W. H. G. Lewin and M. van der Klis (Cambridge University Press, Cambridge, 2006).

[5] H. Schatz, A. Aprahamian, V. Barnard, L. Bildsten, A. Cumming, M. Ouellette, T. Rauscher, F.-K. Thielemann, and M. Wiescher, Phys. Rev. Lett. **86**, 3471 (2001).

[6] L. van Wormer, J. Görres, C. Iliadis, M. Wiescher, and F.-K. Thielemann, Astrophys. J. **432**, 326 (1994).

[7] O. Koike, M. Hashimoto, K. Arai, and S. Wanajo, Astron. Astrophys. **342**, 464 (1999).

[8] B. A. Brown, R. R. C. Clement, H. Schatz, A. Volya, and W. A. Richter, Phys. Rev. C **65**, 045802 (2002).

[9] S. E. Woosley, A. Heger, A. Cumming, R. D. Hoffman, J. Pruet, T. Rauscher, J. L. Fisker, H. Schatz, B. A. Brown, and M. Wiescher, Astrophys. J. Suppl. Ser. **151**, 75 (2004).

[10] J. A. Clark, G. Savard, K. S. Sharma, J. Vaz, J. C. Wang, Z. Zhou, A. Heinz, B. Blank, F. Buchinger, J. E. Crawford, S. Gulick, J. K. P. Lee, A. F. Levand, D. Seweryniak, G. D. Sprouse, and W. Trimble, Phys. Rev. Lett. **92**, 192501 (2004).

[11] G. Savard, R. C. Barber, D. Beeching, F. Buchinger, J. E. Crawford, S. Gulick, X. Feng, E. Hagberg, J. C. Hardy, V. T. Koslowsky, J. K. P. Lee, R. B. Moore, K. S. Sharma, and M. Watson, Nucl. Phys. **A626**, 353 (1997).

[12] J. Clark, R. C. Barber, C. Boudreau, F. Buchinger, J. E. Crawford, S. Gulick, J. C. Hardy, A. Heinz, J. K. P. Lee, R. B. Moore, G. Savard, D. Seweryniak, K. S. Sharma, G. Sprouse, J. Vaz, J. C. Wang, and Z. Zhou, Nucl. Instrum. Methods Phys. Res. B **204**, 487 (2003).

[13] G. Savard, J. Clark, C. Boudreau, F. Buchinger, J. E. Crawford, H. Geissel, J. P. Greene, S. Gulick, A. Heinz, J. K. P. Lee, A. Levand, M. Maier, G. Münzenberg, C. Scheidenberger, D. Seweryniak, K. S. Sharma, G. Sprouse, J. Vaz, J. C. Wang, B. J. Zabransky, Z. Zhou, and the S258 Collaboration, Nucl. Instrum. Methods Phys. Res. B **204**, 582 (2003).

[14] G. Savard, St. Becker, G. Bollen, H.-J. Kluge, R. B. Moore, Th. Otto, L. Schweikhard, H. Stolzenberg, and U. Wiess, Phys. Lett. **A158**, 247 (1991).

[15] G. Bollen, R. B. Moore, G. Savard, and H. Stolzenberg, J. Appl. Phys. **68**, 4355 (1990).

[16] M. König, G. Bollen, H.-J. Kluge, T. Otto, and J. Szerypo, Int. J. Mass Spectrom. Ion Processes **142**, 95 (1995).

[17] G. Gräff, H. Kalinowsky, and J. Traut, Z. Phys. A **297**, 35 (1980).

[18] K. S. Sharma, J. Vaz, R. C. Barber, F. Buchinger, J. A. Clark, J. E. Crawford, H. Fukutani, J. P. Greene, S. Gulick, A. Heinz, J. K. P. Lee, G. Savard, Z. Zhou, and J. C. Wang, Eur. Phys. J. A **25**, s01, 45 (2005).

[19] J. V. F. Vaz, Ph.D. thesis, University of Manitoba, 2002.
[20] G. Savard, J. A. Clark, F. Buchinger, J. E. Crawford, S. Gulick, J. C. Hardy, A. A. Hecht, V. E. Iacob, J. K. P. Lee, A. F. Levand, B. F. Lundgren, N. D. Scielzo, K. S. Sharma, I. Tanihata, I. S. Towner, W. Trimble, J. C. Wang, Y. Wang, and Z. Zhou, Phys. Rev. C **70**, 042501(R) (2004).
[21] G. Savard, F. Buchinger, J. A. Clark, J. E. Crawford, S. Gulick, J. C. Hardy, A. A. Hecht, J. K. P. Lee, A. F. Levand, N. D. Scielzo, H. Sharma, K. S. Sharma, I. Tanihata, A. C. C. Villari, and Y. Wang, Phys. Rev. Lett. **95**, 102501 (2005).
[22] G. Audi, A. H. Wapstra, and C. Thibault, Nucl. Phys. **A729**, 337 (2003).
[23] A. H. Wapstra, G. Audi, and C. Thibault, Nucl. Phys. **A729**, 129 (2003).
[24] G. Audi and A. H. Wapstra, Nucl. Phys. **A595**, 409 (1995).
[25] P. Möller, J. R. Nix, W. D. Myers, and W. J. Swiatecki, At. Data Nucl. Data Tables **59**, 185 (1995).
[26] G. F. Lima, A. Lépine-Szily, G. Audi, W. Mittig, M. Chartier, N. A. Orr, R. Lichtenthaler, J. C. Angelique, J. M. Casandjian, A. Cunsolo, C. Donzaud, A. Foti, A. Gillibert, M. Lewitowicz, S. Lukyanov, M. MacCormick, D. J. Morrissey, A. N. Ostrowski, B. M. Sherrill, C. Stephan, T. Suomijarvi, L. Tassan-Got, D. J. Vieira, A. C. C. Villari, and J. M. Wouters, Phys. Rev. C **65**, 044618 (2002).
[27] C. N. Davids and D. R. Goosman, Phys. Rev. C **7**, 122 (1973).
[28] M. Chartier, M. B. Gómez Hornillos, W. Mittig, A. Lépine-Szily, L. Caballero Ontanaya, C. E. Demonchy, G. Georgiev, N. A. Orr, G. Politi, M. Rousseau, P. Roussel-Chomaz, and A. C. C. Villari, J. Phys. G **31**, S1771 (2005).
[29] T. Rauscher and F. -K.Thielemann, At. Data Nucl. Data Tables **75**, 1 (2000).
[30] G. Audi, O. Bersillon, J. Blachot, and A. H. Wapstra, Nucl. Phys. **A729**, 3 (2003).